Compositional Characterization of Inclusion/Matrix Boundaries and Relation to Pit Initiation at MnS in Stainless Steel

Masayuki Tohjoh, Izumi Muto, Aya Chiba, Yu Sugawara, Nobuyoshi Hara

Department of Materials Science, Tohoku University
6-6-02, Aramaki, Aoba-ku, Sendai 980-8579, Japan

Non-metal inclusions, such as MnS, in stainless steels are major initiation sites of pitting corrosion in chloride environments. In previous studies [1,2], it was found that pitting is initiated at MnS/steel boundaries in NaCl solutions. It is important to make clear the relationship between the electrochemical properties and the compositional characteristics of the MnS/steel boundaries. Microscopic polarization measurements and electron microscopic observation of the MnS/steel boundaries were conducted.

Two re-sulfurized (0.025 mass% S) stainless steels (steels A and B) were prepared by vacuum induction melting. The chemical composition of steel A was equivalent to Type 304L. Steel B was N-containing 304L (0.12 mass% N). Small sulfide inclusions, which mainly consist of Mn and S, were generated in the steels. The specimens were heat-treated at 1373K for 1.8 ks and water-quenched. The specimen surfaces were polished up to 1 μm diamond paste. Microelectrochemical polarization measurements were performed in a 0.1 M NaCl solution at 298 K under naturally aerated conditions.

Figure 1 shows microscopic polarization curves of the small areas (*ca*. 70 μm × *ca*. 100 μm) with the MnS inclusions of steels A and B. A broad current increase was observed at 0.4 V in steel A, and then a current spike occurred at around 0.45 V. This current spike corresponds to metastable pit initiation. No current increase was observed at around 0.45 V in steel B, suggesting that the MnS inclusions in this steel did not dissolve electrochemically. A stable pit occurred at 1.07 V. The difference in pitting corrosion resistance of steels A and B was thought to be associated with the chemical composition of the inclusions and/or the inclusion/steel boundaries.

Figure 2 shows the elemental mapping and the scanning electron microscopy images of the MnS after the polarization measurements. Pits were generated at the MnS/steel boundaries in steels A and B. The existence of C, Cr, O, and S was observed on the inclusion surface of steel A. In the case of steel B, the signals of C, Mn, O, and S were detected on the inclusion surface. It is thought that C and/or O on the inclusion surface after polarization measurements in steel B influenced corrosion resistance of inclusion and inclusion/steel boundaries.

Figure 3 shows the transmission electron microscopy and electron energy-loss spectrum images of the MnS/steel boundaries of steels A and B after the polarization measurements. In both of steels, the MnS inclusions have the thin film layer at the MnS/steel boundaries. A small amount of C and Cr were accumulated in the layers. It is thought that the property of the thin film layers existed at the MnS/steel boundaries affects the dissolution and the pit initiation behavior of the MnS inclusions.

1. I. Muto, Y. Izumiyama, and N. Hara, *J. Electrochem. Soc*., **154**, C439-C444, (2007).
2. A. Chiba, I. Muto, Yu Sugawara, and N. Hara, *J. Electrochem. Soc*., **159**, C341-C350 (2012).

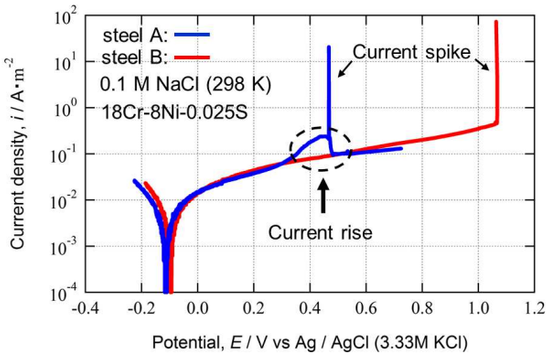

Fig. 1 Microscopic polarization curves of the small areas with MnS inclusions of steels A and B in 0.1 M NaCl at 298 K.

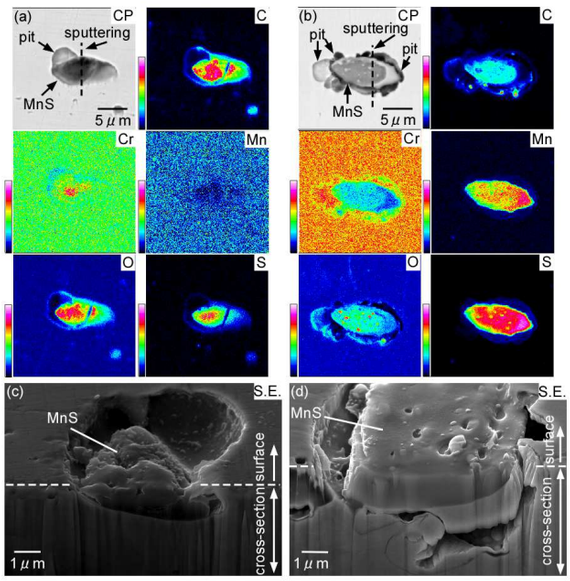

Fig. 2 (a, b) Elemental mapping of MnS surfaces and (c, d) SEM images of the cross-sections of MnS inclusions after the polarization measurements: (a, c) steel A and (b, d) steel B.

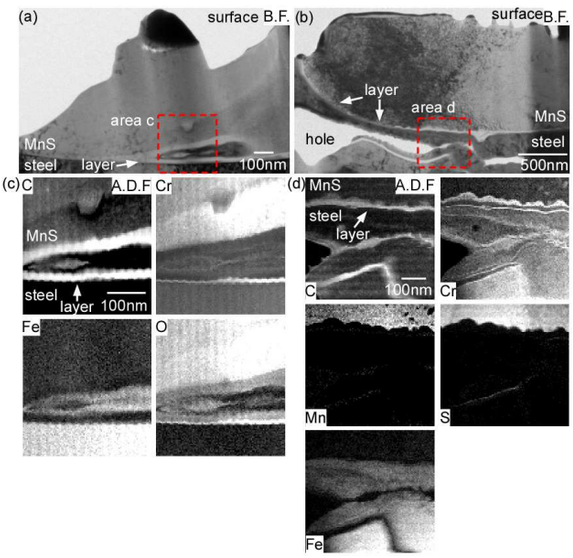

Fig. 3 (a, b) TEM images and EELS elemental mapping of MnS inclusions after the polarization measurements: (a, c) steel A and (b, d) steel B.